Spatial coherence of weakly interacting one-dimensional nonequilibrium bosonic quantum fluids

Vladimir N. Gladilin,[1,2] Kai Ji,[1] and Michiel Wouters[1]
[1]*TQC, Universiteit Antwerpen, Universiteitsplein 1, B-2610 Antwerpen, Belgium*
[2]*INPAC, KU Leuven, Celestijnenlaan 200D, B-3001 Leuven, Belgium*
(Received 29 November 2013; revised manuscript received 11 June 2014; published 11 August 2014)

We present a theoretical analysis of spatial correlations in a one-dimensional driven-dissipative nonequilibrium condensate. Starting from a stochastic generalized Gross-Pitaevskii equation, we derive a noisy Kuramoto-Sivashinsky equation for the phase dynamics. For sufficiently strong interactions, the coherence decays exponentially in close analogy to the equilibrium Bose gas. When interactions are small on a scale set by the nonequilibrium condition, we find through numerical simulations a crossover between a Gaussian and exponential decay with peculiar scaling of the coherence length on the fluid density and noise strength.

DOI: 10.1103/PhysRevA.90.023615 PACS number(s): 67.85.Hj, 71.36.+c

I. INTRODUCTION

The spatial coherence is one of the key observables of quantum degenerate Bose gases. While for Bose gases in thermal equilibrium, its behavior is thoroughly understood [1], the case of nonequilibrium Bose gases has received much less attention. The nonequilibrium condition is typically of importance for photonic systems, where due to the limited reflectivity of any real mirrors, the photon lifetime is usually too short to achieve true thermal equilibrium. A steady state arises instead, thanks to the balancing of external pumping and losses. Also in the nonequilibrium situation, the spatial coherence remains a central observable that is experimentally accessible for photons [2]. Despite the existence of spatially extended lasers for many decades [3], the interest in the fundamental properties of nonequilibrium quantum fluids has come quite recently, with the advent of microcavity polariton quantum fluids [4]. Polaritons are the quasiparticles that arise from the strong coupling between a photon mode and an excitonic excitation in a quantum well. They inherit the good coherence properties from the photon together with substantial interactions from the exciton. Experimentally, spatial coherence measurements have been performed for two-dimensional polariton quantum fluids by many groups [2,5–8].

In most experiments with microcavity polaritons, the nonequilibrium condition is essential to understand their properties. It gives for instance rise to a flow in the steady state [8–10], which can assume the form of quantized vortices [11] or feature more complicated patterns [12]. From the theoretical point of view, these nonequilibrium flows can be understood on a mean-field level, from a generalized Gross-Pitaevskii equation (gGPE) [13,14], that is of the same type as the complex Ginzburg-Landau equation. In this paper, we will consider an equation in the form [4]

$$i\hbar\frac{\partial}{\partial t}\psi = \left[-\frac{\hbar^2\nabla^2}{2m} + g|\psi|^2 + \frac{i}{2}\left(\frac{P}{1+|\psi|^2/n_s} - \gamma\right)\right]\psi. \tag{1}$$

Here m is the effective mass and interactions are described by a contact interaction with strength g. The imaginary term in the square brackets on the right-hand side describes the saturable pumping (with strength P and saturation density n_s) that compensates for the losses (γ). The physical origin of the pumping term for exciton-polariton condensates is an excitonic reservoir that is excited by a nonresonant laser. For the case of ordinary lasing in the weak-coupling regime, it describes emission of photons from the inverted electronic transition. In laser physics, a wide variety of spatial optical patterns, described by gGP-like equations, has been observed [3].

In this work, we investigate the first-order coherence function at long distances. For the description of the spatial coherence, fluctuations have to be added to the gGPE. We will consider the simplest case of spatially uncorrelated and spectrally white additive noise. We thus supplement the right-hand side of the gGPE with a stochastic term $\sqrt{D}dW/dt$, where the complex stochastic increments have the correlation function $\langle dW^*(x,t)dW(x',t')\rangle = 2\delta(x-x')\delta_{t,t'}dt$. The coefficient D describes the strength of the fluctuations. The contributions from quantum fluctuations can for example be derived within a truncated Wigner approximation, leading to $D \sim \gamma$ [15].

In Sec. II, we will derive a nonlinear equation for the stochastic evolution of the phase that is of the form of a noisy Kuramoto-Sivashinsky equation (KSE). The asymptotic behavior of the first-order coherence is investigated in Sec. III. Especially the case of vanishing elastic interaction constant g turns out to be strongly affected by the nonlinearity in the KSE. It is studied by means of numerical simulations. Conclusions are drawn in Sec. IV.

II. THE PHASE EQUATION

In homogeneous systems, a simple uniform steady state solution of Eq. (1) exists. When the pumping exceeds the losses ($P > \gamma$), it reads $\psi_0 = \sqrt{n_0}e^{-i\mu t/\hbar}$, where $n_0 = n_s(P/\gamma - 1)$ and the oscillation frequency is determined by the interaction energy $\mu = gn_0$.

As usual for the calculation of the coherence of a low-dimensional system, we perform the Madelung transformation $\psi = \sqrt{n}e^{i\theta}$ to describe the complex field in terms of its density and phase. This is most convenient, because the long-range part of the spatial coherence is dominated by phase fluctuations. In the regime of weak noise, the density fluctuations are small and we can expand the interaction and gain saturation terms up to linear order in $\delta n = n - n_0$. Because the low-momentum density fluctuations relax much

faster than the long-wavelength phase fluctuations, they can be adiabatically eliminated to derive an equation of the phase dynamics only.

Inserting $\psi = \sqrt{n_0 + \delta n} e^{i\theta - i\mu t/\hbar}$ with $|\delta n| \ll n_0$ into Eq. (1), supplemented with a stochastic term $\sqrt{D} dW/dt$, and neglecting terms of second order in $(\delta n/n_0)$, one obtains

$$\frac{\hbar}{2}\frac{\partial}{\partial t}\frac{\delta n}{n_0} = -\frac{\hbar^2}{2m}\left[\nabla\frac{\delta n}{n_0}\nabla\theta + \left(1+\frac{\delta n}{n_0}\right)\nabla^2\theta\right] - \frac{1}{2\eta}\frac{\delta n}{n_0} + \sqrt{\frac{D}{n_0}}\frac{dW_n}{dt}, \tag{2}$$

$$\hbar\frac{\partial}{\partial t}\theta = \frac{\hbar^2}{2m}\left[\frac{1}{2}\nabla^2\frac{\delta n}{n_0} - \left(\nabla\theta\right)^2\right] - \mu\frac{\delta n}{n_0} + \sqrt{\frac{D}{n_0}}\frac{dW_\theta}{dt}, \tag{3}$$

where the real stochastic variables dW_n and dW_θ have correlators $\langle dW_n(x,t)dW_n(x',t')\rangle = \langle dW_\theta(x,t)dW_\theta(x',t')\rangle = \delta(x-x')\delta_{t,t'}dt$. Assuming that the characteristic time $\eta = (1+n_s/n_0)\gamma^{-1}$, which determines relaxation of density fluctuations, is sufficiently short, the quantity $\delta n/n_0$ can be estimated from Eq. (2) as

$$\frac{\delta n}{n_0} \approx -\frac{\hbar^2\eta}{m}\nabla^2\theta + 2\eta\sqrt{\frac{D}{n_0}}\frac{dW_n}{dt}. \tag{4}$$

When inserting $\delta n/n_0$ given by Eq. (4) into Eq. (3), we take into account that at small η values under consideration (i) the inequality $\eta|\mu| \ll 1$ is satisfied for a moderate interaction strength and (ii) the contribution $\hbar^2\eta(2m)^{-1}\sqrt{D/n_0}\nabla^2(dW_n/dt)$ to the noise term can be neglected (except for the shortest length scale, which we are not interested in). Then one obtains for the phase equation the expression

$$\hbar\frac{\partial}{\partial t}\theta = \frac{\hbar^2}{2m}\left[-\frac{\hbar^2\eta}{2m}\nabla^4\theta - (\nabla\theta)^2 + 2\eta\mu\nabla^2\theta\right] + \sqrt{\frac{D}{n_0}}\frac{dW_\theta}{dt}. \tag{5}$$

In Appendix A, we corroborate the equivalence of the phase equation (5) and the full Gross-Pitaevskii equation (1) with numerical simulations. In the case of stronger interactions, when the inequality $\eta|\mu| \ll 1$ is violated, one should simply replace the noise strength D in Eq. (5) [as well as in Eqs. (3) to (6)] with $D(1+2\eta\mu)^2$.

For the analysis, it is useful to write the phase equation in dimensionless form, by the rescalings $x = l_*\tilde{x}$, $t = t_*\tilde{t}$, and $\theta = \theta_*\tilde{\theta}$, where the length scale equals

$$l_* = \left(\frac{\hbar^2}{2m}\right)^{4/7}\eta^{3/7}\left(\frac{D}{\hbar n_0}\right)^{-1/7}. \tag{6}$$

Note its very weak dependence on the physical parameters n_0 and D. The time and phase scales read

$$t_* = \hbar\left(\frac{\hbar^2}{2m}\right)^{2/7}\eta^{5/7}\left(\frac{D}{\hbar n_0}\right)^{-4/7}, \tag{7}$$

$$\theta_* = \left(\frac{\hbar^2}{2m}\right)^{-1/7}\eta^{1/7}\left(\frac{D}{\hbar n_0}\right)^{2/7}. \tag{8}$$

They depend on the density relaxation time η, which decreases in our saturable gain model (1) for increasing density n_0. The interaction energy, rescaled as $\tilde{\mu} = \mu/\mu_*$ where

$$\mu_* = \frac{1}{2}\left(\frac{\hbar^2}{2m}\right)^{-1/7}\eta^{-6/7}\left(\frac{D}{\hbar n_0}\right)^{2/7}, \tag{9}$$

remains as the only control parameter in the dimensionless phase equation

$$d\tilde{\theta} = \left[\tilde{\mu}\nabla_{\tilde{x}}^2\tilde{\theta} - \nabla_{\tilde{x}}^4\tilde{\theta} - (\nabla_{\tilde{x}}\tilde{\theta})^2\right]d\tilde{t} + d\tilde{W}. \tag{10}$$

Here, the increment $d\tilde{W}$ in Eq. (10) is a real stochastic variable with correlation function $\langle d\tilde{W}(\tilde{x},\tilde{t})d\tilde{W}(\tilde{x}',\tilde{t}')\rangle = \delta(\tilde{x}-\tilde{x}')\delta_{\tilde{t},\tilde{t}'}dt$.

Note that in the absence of gain saturation $\eta \to \infty$ (obtained in the limit $\gamma \to 0$), the time scale t_* diverges. The physical reason is that gain saturation is the only damping mechanism in our model. We have verified that a small energy relaxation term [16] does not have a qualitative impact on the results presented below.

The phase equation (10) is of the form of the noisy Kuramoto-Sivashinsky equation (KSE) [17]. The KSE equation has a wide range applications, covering, e.g., flame fronts [18] and reaction-diffusion systems [19], as well as transverse pattern formation in lasers [20,21].

The noisy KSE (10) has been studied in the context of kinetic surface roughening [22]. It has been shown [23] that it belongs to the universality class of the celebrated Kardar-Parisi-Zhang (KPZ) equation [24] (Eq. (10) without the fourth-order derivative; for a review, see [25]). To the best of our knowledge, the spatial correlations of the noisy KSE have however not been systematically analyzed as a function of the control parameter $\tilde{\mu}$.

III. LONG-RANGE SPATIAL COHERENCE

A. Repulsive interactions

Let us start with the case of repulsive interactions $\tilde{\mu} > 0$. In equilibrium, this is the only meaningful case because attractive interactions lead to a collapse. The linearized version of Eq. (10) is then a good starting point to understand the momentum distribution. It reads

$$\langle|\tilde{\theta}_{\tilde{k}}|^2\rangle = \frac{1}{2(\tilde{\mu}\tilde{k}^2 + \tilde{k}^4)}, \tag{11}$$

where $\tilde{k} = kl_*$ is the rescaled momentum. The denominator represents the square of the Bogoliubov excitation spectrum $\tilde{\omega}_B^2(k) = \tilde{\mu}\tilde{k}^2 + \tilde{k}^4$.

The quadratic term dominates for wave vectors $\tilde{k} < \sqrt{\tilde{\mu}}$. In this region, the phase dynamics reduces to the KPZ equation, which was used for polaritons by Altman *et al.* [26]. Its relevance in the context of equilibrium quantum fluids was also pointed out in recent works on the dynamical structure factor of 1D bosons, both in the weakly [27] and the strongly [28] interacting limits.

So far, the discussion is valid for arbitrary dimensionality, but now we will restrict ourselves to a one-dimensional system,

where the nonlinear term in the KPZ equation leaves the solution of the linearized equation invariant. The momentum distribution of the phase field is then given by Eq. (11). This corresponds to the quadratically decaying momentum distribution at long wavelengths as in 1D finite temperature equilibrium condensates. Equation (11) implies with the Fourier relation

$$\overline{\delta\theta^2}(x) = \frac{1}{L}\sum_k \langle|\theta_k|^2\rangle[\cos(kx) - 1] \tag{12}$$

that the phase-phase correlator decreases for long distances linearly with the distance

$$\overline{\delta\tilde{\theta}^2}(x) \equiv \langle\tilde{\theta}(x)\tilde{\theta}(0)\rangle - \langle\tilde{\theta}^2(0)\rangle = -\tilde{x}/(4\tilde{\mu}). \tag{13}$$

For the evaluation of the characteristic function that determines the shape of the spatial coherence function $g^{(1)}(x) = \langle\psi^\dagger(x)\psi(0)\rangle$, the second cumulant approximation is exact thanks to the Gaussian nature of the phase field in the solution of the KPZ equation [25]. For the correlation length in the exponential decay

$$g^{(1)}(x) \approx n_0\langle\exp\{i[\theta(x) - \theta(0)]\}\rangle \tag{14}$$

$$= n_0 \exp\left[-\frac{x\,Dm}{4\hbar^2 n\eta\mu}\right], \tag{15}$$

we then recover the expression for the coherence length $\ell_c = 4\hbar^2 n\eta\mu/(Dm)$, which was derived in Ref. [29]. An appealing correspondence with the equilibrium case [$\ell_c^{\text{eq.}} = 2n\hbar^2/(k_B T m)$] can be made by identifying the temperature T with the noise strength and the mass with the "effective mass" $m\eta/\mu$ that quantifies the curvature of the imaginary part of the dispersion. It should be understood however that this formal analogy between the equilibrium and nonequilibrium cases is not sufficient to identify the noise strength D with an effective temperature. For the identification of a proper temperature at long length scales for the driven-dissipative Bose gases, we refer to the renormalization-group study in Ref. [30].

B. Zero interaction strength

A salient feature of coherence length is that it tends to zero in the absence of interactions. The linearized theory thus leads to the prediction that a repulsive nonlinearity is essential for the spatial coherence of a nonequilibrium condensate or a laser. The problem for vanishing interactions can be immediately seen from Eqs. (11) and (12), because the sum over momenta features an infrared divergence, due to the k^{-4} divergence of the momentum distribution.

In this case however, the nonlinear term in Eq. (10) does not keep the momentum distribution (11) obtained in the linearized approximation invariant. We can expect on the basis of a previous analysis [23] of the noisy KSE that the nonlinear term actually keeps the system in the KPZ universality class, featuring a k^{-2} behavior of the momentum distribution. In order to investigate the spatial coherence for smaller interaction energy, we have performed numerical simulations.

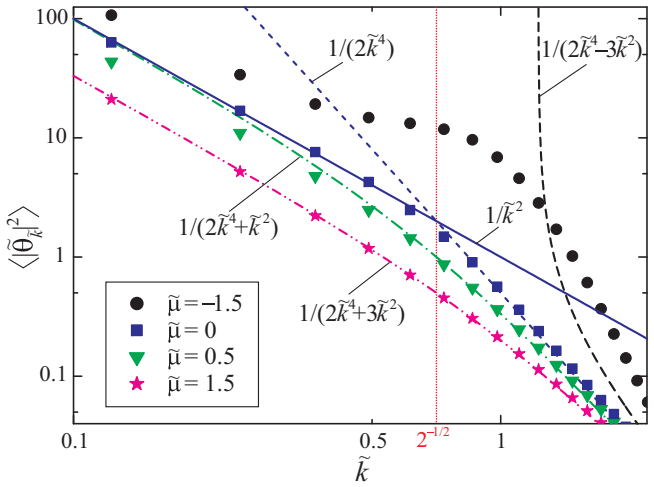

FIG. 1. (Color online) Numerically calculated momentum distribution of the phase field, $\langle|\tilde{\theta}_{\tilde{k}}|^2\rangle$, as a function of $\tilde{k}$ for $\tilde{\mu} = -1.5$ (circles), 0 (squares), 0.5 (triangles), and 1.5 (stars). The dashed, short-dashed, dash-dotted, and dash-dot-dotted curves represent the momentum distribution given by Eq. (11) for $\tilde{\mu} = -1.5$, 0, 0.5, and 1.5, respectively. The function $\tilde{k}^{-2}$ (solid line) approximates the calculated low-momentum behavior of $\langle|\tilde{\theta}_{\tilde{k}}|^2\rangle$ in the absence of interactions. The dotted vertical line corresponds to the crossover between this behavior and a faster ($\propto \tilde{k}^{-4}$) decay at higher momenta.

Figure 1 presents the momentum distribution of the phase field for various values of the interaction energy. Our numerics confirms the validity of the linearized approximation (11) for sufficiently strong repulsive interactions by the excellent agreement between the stars and the dash-dot-dotted line for $\tilde{\mu} = 1.5$. This corresponds to the KPZ regime discussed above, where the nonlinearity of Eq. (10) does not affect the static correlation function. For the intermediate interaction strength on the other hand, pronounced differences between the linearized approximation (dash-dotted) and the numerical simulations (triangles) become apparent at low k.

For zero interaction strength, the discrepancy between the squares and the dashed line is dramatic: instead of the k^{-4} behavior predicted by the linearized approximation, the momentum distribution exhibits the same k^{-2} divergence as in the KPZ interacting regime. The prefactor in the low-momentum region turns out to be 1 within our numerical accuracy of a few percent. As can be seen from Fig. 1, for $\tilde{\mu} = 0$ the piecewise approximation to the momentum distribution

$$\langle|\tilde{\theta}_{\tilde{k}}|^2\rangle = \begin{cases} \tilde{k}^{-2} & \text{for } \tilde{k} < 1/\sqrt{2} \\ \frac{1}{2}\tilde{k}^{-4} & \text{for } \tilde{k} > 1/\sqrt{2} \end{cases} \tag{16}$$

is excellent for almost all $\tilde{k}$, thanks to the sharp crossover between the $\tilde{k}^{-4}$ and $\tilde{k}^{-2}$ regions. This should be contrasted with the much smoother crossover—described by the analytic function (11)—for strong repulsive interactions (pink stars).

The scaled phase-phase correlator in real space is shown in Fig. 2. The large-distance ($\tilde{x} \gg 1$) decay is dominated by the $\tilde{k}^{-2}$ region in the Fourier expansion (12) and reads

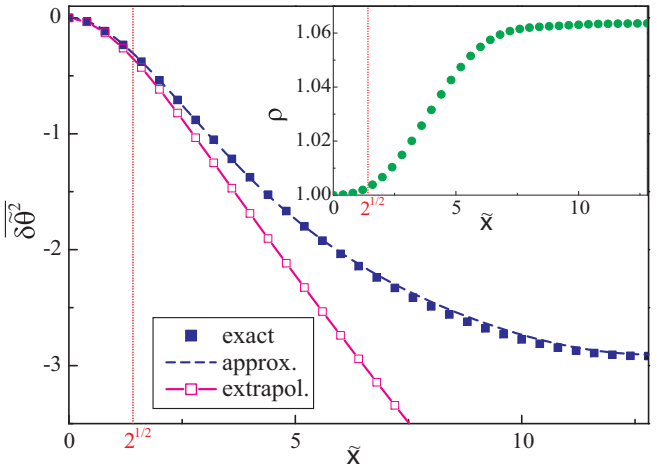

FIG. 2. (Color online) Phase-phase correlator in real space for $\tilde{\mu} = 0$, $L = 25.6 l_*$ as given by the numerical simulations (full squares) and by the analytical formula resulting from the piecewise approximation (16) (dashed curve). The finite-size correction described by this formula has been used to extrapolate the numerical data to the case $L \to \infty$ (open squares). Inset: Ratio $\rho(x) = \ln\langle\exp\{i[\theta(x) - \theta(0)]\}\rangle / \overline{\delta\theta^2}(x)$ calculated numerically for $\tilde{\mu} = 0$, $\theta_* = 1$, $L = 25.6 l_*$.

in the continuum limit $\overline{\delta\tilde{\theta}^2}(\tilde{x}) = -\tilde{x}/2$. The short-range phase fluctuations are obtained by expanding the cosine in Eq. (12) up to second order. It turns out that the low and high momentum regions contribute equally. The piecewise momentum distribution (16) leads to $\overline{\delta\tilde{\theta}^2}(\tilde{x}) = -\tilde{x}^2/\sqrt{2\pi^2}$, valid for $\tilde{x} \ll 1$. Within the second cumulant approximation, this leads to successive Gaussian and exponential decays for the first-order spatial coherence function $g^{(1)}(x)$. The border between both regimes is determined by the length scale l_*.

In the exponential regime, we find for the correlation length $l_e = 2 l_* \theta_*^{-2}$, featuring the peculiar scalings as a function of the physical quantities $l_e \propto n_0^{5/7} D^{-5/7} m^{-6/7} \eta^{1/7}$. Note the different scalings as a function of the physical parameters as compared to the regime of strong interactions. The Gaussian correlation length is $l_G = (2\pi^2)^{1/4} l_* \theta_*^{-1} \eta^{2/7}$ and scales as $l_G \propto n_0^{3/7} D^{-3/7} m^{-5/7}$. When the initial Gaussian decay is by many orders of magnitude, the long-distance exponential tail becomes irrelevant. It is then meaningful to distinguish two regimes. The decay is dominantly Gaussian when the "phase scale" θ_* is much larger than one, where it is dominantly exponential in the opposite limit. In terms of the physical parameters of the nonequilibrium Bose fluid, the decay is dominantly Gaussian for large noise and low density: $D > \hbar^2 n_0 / \sqrt{2\eta m}$.

Thanks to the sharp crossover of the momentum distribution between its two limiting behaviors, the piecewise approximation (16) actually leads to an accurate expression for the phase correlator at all distances. Its explicit form is given in Appendix B. In Fig. 2, it is displayed with a dotted line, showing almost perfect agreement with the numerical results. Furthermore, the analytic formula allows us to do a straightforward extrapolation to infinite systems (open squares in Fig. 2). The good agreement between extrapolations starting from simulations with different sizes (not shown here) confirms good convergence of our results as a function of system size.

The above analysis was based on the assumption of the validity of the second cumulant approximation for the characteristic function $\langle\exp\{i[\theta(x) - \theta(0)]\}\rangle$. It is obviously applicable for small phase variations, when this correlator is well approximated by an expansion of the exponentials up to the second order in θ. For Gaussian phase fluctuations, it is also guaranteed to hold, thanks to Wick's theorem. For the short-wavelength fluctuations, the nonlinear term can be neglected, so that the phase increments are a linear combination of the input noise, and therefore guaranteed to be Gaussian by the central limit theorem. For the long-wavelength components, which are crucially affected by the nonlinearity, the situation is more complicated and the corresponding results of our numerical calculations are somewhat less conclusive. For large distances x the calculated values of the characteristic function $\langle\exp\{i[\theta(x) - \theta(0)]\}\rangle$ appear to be slightly lower than those given by the second-cumulant expression $\exp\{\overline{\delta\theta^2}(x)\}$. In the inset to Fig. 2, we plot the ratio $\rho(x) = \ln\langle\exp\{i[\theta(x) - \theta(0)]\}\rangle / \overline{\delta\theta^2}(x)$ obtained for $\theta_* = 1$. Starting from $\rho = 1$ at $x \ll l_*$, this ratio slightly increases at $x \gtrsim \sqrt{2} l_*$ and apparently tends to saturate at even larger x. It is worth mentioning that the statistical convergence of the calculation of the correlator $\langle\exp\{i[\theta(x) - \theta(0)]\}\rangle$, especially for relatively large x, is much slower as compared to the calculation of the phase fluctuations $\overline{\delta\theta^2}$. However, we find systematic and consistent deviations from Gaussian statistics both in the correlator $\langle\exp\{i[\theta(x) - \theta(0)]\}\rangle$ and in the fourth cumulant of the phase fluctuations. As can be seen from the inset in Fig. 2, for the chosen value $\theta_* = 1$, which corresponds to a rather strong noise, the difference is only $\rho(x) - 1 \approx 0.06$.

C. Attractive interactions

Finally, we briefly discuss the case of attractive interactions. The equilibrium Bose gas is unstable with respect to the collapse of the gas because of the negative compressibility. The nonequilibrium counterpart is reflected in the linear instability of Eq. (10) for $\tilde{\mu} < 0$. In the nonequilibrium case however, the nonlinear term has a stabilizing effect, leading merely to a modulation of the phase (and correspondingly of the density) instead of a collapse. It is well known that for $\tilde{\mu} < 0$, the KSE without noise shows chaotic behavior, leading to effective stochastic dynamics at large scales, where the stochastic driving force stems from the linear instability [25]. The deterministic KSE with $\tilde{\mu} < 0$ and the stochastic KPZ equation belong to the same universality class [31]. Adding a stochastic term preserves this correspondence [23]. The dots in Fig. 1 show a momentum distribution for moderately attractive interactions ($\tilde{\mu} = -1.5$). The bump around $\tilde{k} = 1$ also appears in the absence of the noise [32] and corresponds in real space to a modulation of the phase. At small momenta, the momentum distribution shows the same k^{-2} behavior as in the case of repulsive or zero interactions, leading again to an exponential decay at the longest distance scales.

IV. CONCLUSIONS

In conclusion, we have shown that the coherence of a nonequilibrium Bose gas is governed by the noisy Kuramoto-Sivashinsky equation and we have analyzed the effect of interactions. In contrast to linearized Bogoliubov theory, our study has shown that the coherence length does not vanish when interactions tend to zero, even though it is shorter than in the case of repulsive interactions. Our approach is also applicable to the case of attractive interactions, where phase fluctuations are enhanced by the modulational instability of the condensate. For very strong repulsive interactions on the other hand, where the system approaches the Tonks-Girardeau regime, our mean-field approximation breaks down and more sophisticated techniques should be used [33]. Our predictions could be verified experimentally in semiconductor microcavities, where the repulsive interaction strength can be varied by changing the exciton-photon detuning [34].

ACKNOWLEDGMENTS

We acknowledge stimulating discussions with Iacopo Carusotto and Jacques Tempere. This work was financially supported by the FWO Odysseus program.

APPENDIX A: IMPACT OF PHASE CORRELATIONS ON THE FIELD-FIELD CORRELATOR

In Fig. 3 we compare the functions $\exp[\overline{\delta\theta^2}(x)]$, obtained by rescaling the phase correlator $\overline{\delta\tilde{\theta}^2}(\tilde{x})$ (see the paper), to the the first-order spatial coherence function $g^{(1)}(x)/n_0$, calculated directly from Eq. (1), for the case of $g = 0$, $n_0 = n_s$, and three different values of the noise strength D. While at weak noise (up to $D/D_0 \sim 10^{-3}$) the behavior of the field-field correlator $g^{(1)}(x)$ is perfectly described by the phase factor $\exp[\overline{\delta\theta^2}(x)]$,

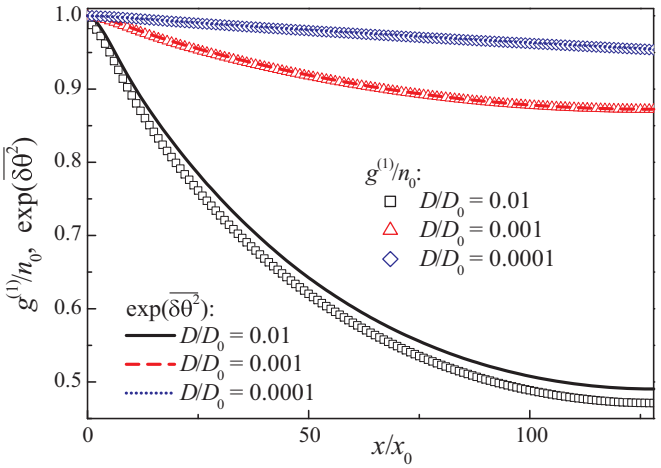

FIG. 3. (Color online) First-order spatial coherence function $g^{(1)}(x)$ calculated numerically from Eq. (1) (open symbols) and the function $\exp[\overline{\delta\theta^2}(x)]$ (lines) for three different values of the noise strength D. The system size is $L = 1024x_0$ in the case of $D/D_0 = 0.0001$ and $L = 256x_0$ for the other two values of D/D_0. Here $x_0 = \sqrt{\hbar n_s/(m\gamma n_0)}$, $D_0 = \hbar^3 n_0/(4mx_0)$.

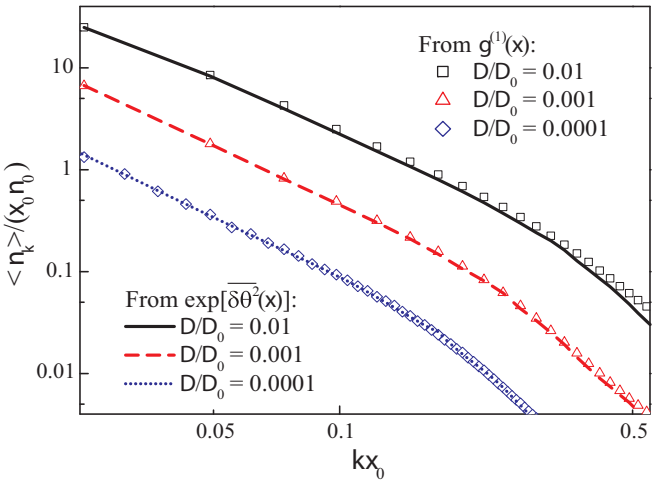

FIG. 4. (Color online) Momentum distribution functions calculated from the filed-field correlator $g^{(1)}(x)$ (open symbols) and from the functions $\exp[\overline{\delta\theta^2}(x)]$ (lines) for three different values of the noise strength D. The system size is $L = 1024x_0$ in the case of $D/D_0 = 0.0001$ and $L = 256x_0$ for the other two values of D/D_0. Here $x_0 = \sqrt{\hbar n_s/(m\gamma n_0)}$, $D_0 = \hbar^3 n_0/(4mx_0)$.

at higher noise strength an additional suppression of $g^{(1)}(x)/n_0$ by density fluctuations becomes nonnegligible. Nevertheless, even in the case of $D/D_0 = 10^{-2}$ where the magnitude of density fluctuations is comparable to n_0, the decay of $g^{(1)}(x)/n_0$ at large distances is seen to be dominated by the effect of phase fluctuations.

In Fig. 4 we plot the momentum distribution functions, which correspond to $g^{(1)}(x)$ (open symbols) and $\exp[\overline{\delta\theta^2}(x)]$ (lines). In line with the discussion above, the long-wavelength behavior of the momentum distribution obtained by solving the "full" field equation (1) is completely determined by phase fluctuations. The effect of (short-range) density fluctuations is manifested only for relatively large momenta at sufficiently high noise strength.

APPENDIX B: FITTING FORMULA FOR THE PHASE-PHASE CORRELATOR

We use the piecewise approximation of Eq. (10) for the momentum distribution $\langle|\tilde{\theta}_{\tilde{k}}|^2\rangle$ in the absence of interactions. Then for a finite system of (dimensionless) size $\tilde{L}$ the scaled phase-phase correlator in real space can be represented as

$$\overline{\delta\tilde{\theta}^2}(\tilde{x}) \approx \frac{\tilde{L}}{2\pi^2}\left[\sum_{\kappa=1}^{\infty}\frac{\cos(2\pi\kappa\tilde{x}/\tilde{L})-1}{\kappa^2} - \sum_{\kappa=\tilde{L}/(2\sqrt{2}\pi)}^{\infty}\frac{\cos(2\pi\kappa\tilde{x}/\tilde{L})-1}{\kappa^2}\right] + \frac{\tilde{L}^3}{(2\pi)^4}\sum_{\kappa=\tilde{L}/(2\sqrt{2}\pi)}^{\infty}\frac{\cos(2\pi\kappa\tilde{x}/\tilde{L})-1}{\kappa^4}. \quad \text{(B1)}$$

Assuming that the system size is sufficiently large, $\tilde{L}/(2\sqrt{2}\pi) \gg 1$, the last two sums in Eq. (B1) can be approximated by the corresponding integrals:

$$\overline{\delta\tilde{\theta}^2}(\tilde{x}) \approx \frac{\tilde{L}}{2\pi^2}\sum_{\kappa=1}^{\infty}\frac{\cos(2\pi\kappa\tilde{x}/\tilde{L})-1}{\kappa^2} - \frac{\tilde{x}}{\pi}\int_{\tilde{x}/\sqrt{2}}^{\infty}dy\,\frac{\cos(y)-1}{y^2} + \frac{\tilde{x}^3}{2\pi}\int_{\tilde{x}/\sqrt{2}}^{\infty}dy\,\frac{\cos(y)-1}{y^4}. \quad \text{(B2)}$$

These integrals as well as the infinite series in Eq. (B2) can be easily evaluated [35] giving finally

$$\overline{\delta\tilde{\theta}^2}(\tilde{x}) = -\frac{\tilde{x}}{2}\left[1+\frac{2}{\pi}\mathrm{si}\left(\frac{\tilde{x}}{\sqrt{2}}\right)\left(1+\frac{\tilde{x}^2}{12}\right)\right] - \frac{2\sqrt{2}}{3\pi}\left[1-\cos\left(\frac{\tilde{x}}{\sqrt{2}}\right)\left(1+\frac{\tilde{x}^2}{8}\right) + \frac{\tilde{x}}{4\sqrt{2}}\sin\left(\frac{\tilde{x}}{\sqrt{2}}\right)\right] + \frac{\tilde{x}^2}{2\tilde{L}}, \quad \text{(B3)}$$

where $si(x)$ is the sine integral [36]. The last term in Eq. (B3) accounts for the finite size of the system.

[1] L. Pitaevskii and S. Stringari, *Bose-Einstein Condensation* (Clarendon, Oxford, 2003).
[2] J. Kasprzak *et al.*, Nature (London) **443**, 409 (2006).
[3] K. Staliunas and V. J. Sánchez-Morcillo, *Transverse Patterns in Nonlinear Optical Resonators* (Springer, Heidelberg, 2003).
[4] I. Carusotto and C. Ciuti, Rev. Mod. Phys. **85**, 299 (2013).
[5] R. Spano *et al.*, New J. Phys. **14**, 075018 (2012).
[6] H. Deng, G. S. Solomon, R. Hey, K. H. Ploog, and Y. Yamamoto, Phys. Rev. Lett. **99**, 126403 (2007).
[7] E. A. Cerda-Méndez, D. N. Krizhanovskii, M. Wouters, R. Bradley, K. Biermann, K. Guda, R. Hey, P. V. Santos, D. Sarkar, and M. S. Skolnick, Phys. Rev. Lett. **105**, 116402 (2010).
[8] E. Wertz, L. Ferrier, D. D. Solnyshkov, R. Johne, D. Sanvitto, A. Lematre, I. Sagnes, R. Grousson, A. V. Kavokin, P. Senellart, G. Malpuech, and J. Bloch, Nat. Phys. **6**, 860 (2010).
[9] M. Richard, J. Kasprzak, R. Romestain, R. André, and L. S. Dang, Phys. Rev. Lett. **94**, 187401 (2005).
[10] M. Wouters, I. Carusotto, and C. Ciuti, Phys. Rev. B **77**, 115340 (2008).
[11] K. Lagoudakis *et al.*, Nat. Phys. **4**, 706 (2008).
[12] P. Cristofolini, A. Dreismann, G. Christmann, G. Franchetti, N. G. Berloff, P. Tsotsis, Z. Hatzopoulos, P. G. Savvidis, and J. J. Baumberg, Phys. Rev. Lett. **110**, 186403 (2013).
[13] M. Wouters and I. Carusotto, Phys. Rev. Lett. **99**, 140402 (2007).
[14] J. Keeling and N. G. Berloff, Phys. Rev. Lett. **100**, 250401 (2008).
[15] M. Wouters and V. Savona, Phys. Rev. B **79**, 165302 (2009).
[16] L. P. Pitaevskii, Zh. Eksp. Teor. Fiz. **35**, 408 (1958) [Sov. Phys. JETP **35**, 282 (1959)].
[17] R. Cuerno and K. B. Lauritsen, Phys. Rev. E **52**, 4853 (1995).
[18] G. Sivashinsky, Acta Astron. **4**, 1177 (1977).
[19] Y. Kuramoto and T. Tsuzuki, Prog. Theor. Phys. **55**, 356 (1976).
[20] R. Lefever, L. A. Lugiato, W. Kaige, N. B. Abraham, and P. Mandel, Phys. Lett. A **135**, 254 (1989).
[21] G. Huyet, M. C. Martinoni, J. R. Tredicce, and S. Rica, Phys. Rev. Lett. **75**, 4027 (1995).
[22] R. Cuerno, H. A. Makse, S. Tomassone, S. T. Harrington, and H. E. Stanley, Phys. Rev. Lett. **75**, 4464 (1995).
[23] K. Ueno, H. Sakaguchi, and M. Okamura, Phys. Rev. E **71**, 046138 (2005).
[24] M. Kardar, G. Parisi, and Y.-C. Zhang, Phys. Rev. Lett. **56**, 889 (1986).
[25] T. Halpin Healy and Y.-C. Zhang, Phys. Rep. **254**, 215 (1995).
[26] E. Altman, L. M. Sieberer, L. Chen, S. Diehl, and J. Toner, arXiv:1311.0876.
[27] M. Kulkarni and A. Lamacraft, Phys. Rev. A **88**, 021603(R) (2013).
[28] M. Arzamasovs, F. Bovo, and D. M. Gangardt, Phys. Rev. Lett. **112**, 170602 (2014).
[29] A. Chiocchetta and I. Carusotto, Eur. Phys. Lett. **102**, 67007 (2013).
[30] L. M. Sieberer, S. D. Huber, E. Altman, and S. Diehl, Phys. Rev. B **89**, 134310 (2014).
[31] V. S. L'vov, V. V. Lebedev, M. Paton, and I. Procaccia, Nonlinearity **6**, 25 (1993).
[32] K. Sneppen, J. Krug, M. Jensen, C. Jayaprakash, and T. Bohr, Phys. Rev. A **46**, R7351 (1992).
[33] T. Giamarchi, *Quantum Physics in One Dimension* (Oxford University Press, Oxford, 2006).
[34] M. Vladimirova, S. Cronenberger, D. Scalbert, K. V. Kavokin, A. Miard, A. Lemaitre, J. Bloch, D. Solnyshkov, G. Malpuech, and A. V. Kavokin, Phys. Rev. B **82**, 075301 (2010); N. Takemura, S. Trebaol, M. Wouters, M. T. Portella-Oberli, and B. Deveaud, arXiv:1310.6506.
[35] A. P. Prudnikov, Yu. A. Brychkov, and O. I. Marichev, *Integrals and Series*, Vol. 1, Elementary Functions (Gordon and Breach Science Publishers, New York, 1986).
[36] M. Abramowitz and I. A. Stegun, *Handbook of Mathematical Functions with Formulas, Graphs, and Mathematical Tables* (Dover, New York, 1972).